Operational Aspects of the Alberta Severe Weather Outbreak of 29 July 1993

Stephen R. J. Knott and Neil M. Taylor

Prairie Aviation and Arctic Weather Center
Meteorological Service of Canada
Environment Canada
Edmonton, Alberta

Submitted in final form August 2000

Abstract

On 29 July 1993 severe thunderstorms tracked northeastwards across central Alberta resulting in numerous severe weather events including 3 reported tornadoes. Radar imagery was used to associate observed storm structure and evolution with the analyzed synoptic and mesoscale environmental conditions. Available data consisted of upper air charts, sounding data, radar data, and surface observations. Surface observations indicate that a dryline formed over the southwest corner of the province. It is suspected that enhanced convergence in the vicinity of the dryline played a role in the initiation of convection. Propagation of the dryline was associated with significant decreases in dewpoint (~10°C in 2 hours) and veering of the surface winds. Two severe storms formed within 30km of the dryline and in the region where the dryline was oriented in such a way as to enhance low-level convergence.

The 1200 UTC sounding and upper air charts showed a conditionally unstable environment and veering of the low-level winds with relatively unidirectional wind shear aloft. These conditions have been shown to be indicative of potential storm splitting favoring the right-moving storm (Weisman and Klemp 1982, 1986). Two of the four severe storms that developed exhibited classic radar signatures characteristic of splitting storms prior to splitting. The right-moving member of one of these storms later spawned an F3 tornado. By highlighting the synoptic and mesoscale features indicative of dryline formation and storm splitting, we hope to help the severe weather meteorologist anticipate storm genesis and behavior and quickly adapt severe thunderstorm and tornado warning areas accordingly.

Operational Aspects of the Alberta Severe Thunderstorm Outbreak of 29 July 1993

1. Introduction

The release of latent energy in an environment of strong vertical wind shear often leads to the development of severe convective storms. On 29 July 1993 several severe thunderstorms tracked across central Alberta resulting in numerous severe weather events including 3 reported tornadoes (Vickers 1994). In this paper we focus our discussion on interesting operational aspects of this severe weather outbreak: specifically, the presence of a dryline and its role in thunderstorm development, a wind shear environment conducive to splitting severe storms and the subsequent splitting of at least two storms that later produced tornadoes (one of F3 intensity near the town of Holden), and the development of a severe thunderstorm over the city of Edmonton resulting from outflow boundary interactions.

Following an introduction to thunderstorm climatology for Alberta, an overview of drylines and wind shear environments conducive to non-splitting and splitting supercells are presented. We examine the synoptic and mesoscale environmental conditions leading to the severe weather outbreak on 29 July 1993 and the radar observed storm evolution is discussed. We conclude with a discussion highlighting the operational recognition of dryline formation and the potential for storm splitting.

a. Alberta thunderstorm climatology

Central Alberta is highly susceptible to severe thunderstorms during the summer months (e.g., Chisholm and Renick 1972; Chisholm 1973; Smith and Yau 1993). This region experiences an average of 61 hailfall days each summer (Wojtiw 1975) and between 10 and 20 tornadoes annually (Newark 1984; Bullas and Wallace 1988).

Most climatological studies of Alberta thunderstorms stem from data collected during the Alberta Hail Studies Project (ALHAS) and the Alberta Hail Project (AHP) from 1957 to 1985 (see Longley and Thompson 1965; Chisholm 1973; Wojtiw 1975). Longley and Thompson (1965) used hailfall and sounding data to construct composite 850mb and 500mb charts indicative of hail events of differing intensity in central Alberta. In general, an upper trough upstream and closed low over southern Alberta were suggestive of significant hailfall events. Wojtiw (1975) plotted storm tracks of Alberta hailstorms showing a preference for storms to develop over the foothills before migrating northeastwards onto the plains. In addition, he showed July to be the most active month for hail activity in Alberta. Later hailfall climatologies related an increased number of hail reports to larger hailsizes (Smith and Yau 1993) and investigated the episodic nature of significant hailfall events (Smith et al. 1998).

Newark (1984) compiled a climatology of Canadian tornadoes showing the highest annual frequency of tornadoes in the prairies to occur in southern Manitoba with a secondary maximum in south-central Alberta. More recently, McCarthy (1998, personal communication) found an average

of 16 tornadoes to occur annually in Alberta compared to only 9 in Manitoba. Other climatological studies of Alberta storms have examined population density effects on the number of severe weather events reported (Paruk and Blackwell 1994) and lightning distributions (Kozak 1998). Paruk and Blackwell (1994) showed severe thunderstorm event densities to have maxima in the region between (and including) Calgary and Edmonton including the foothills northwest of Calgary (Fig. 1). This area corresponds to a high frequency of hailstorm tracks (Wojtiw 1975) and lightning strikes (Fig. 2) and is an area known among Alberta forecasters to be prone to severe storm development.

b. Forecasting thunderstorms in Alberta

Weather forecasting in Alberta has its challenges. Located in the lee of the Rocky Mountain range, surface wind direction plays an important role in the initiation of summertime convection. Thus, correctly diagnosing the properties of the low-level flow is key to forecasting the weather in this province. The foothills of the Rockies are the primary genesis zone for Alberta thunderstorms due mainly to the effects of differential heating. Conditions conducive to thunderstorm initiation include sunny skies and a northeasterly or easterly surface wind. The climatological dewpoint axis in the prairies (Fig. 3) lies to the east of the foothills with dewpoint maxima extending from southeast Manitoba (near Winnipeg) to near Edmonton in central Alberta with the driest air in the vicinity of the foothills. Therefore, not only does a northeasterly surface wind provide an upslope component for lift in the foothills, it typically advects relatively moist boundary layer air into the foothills beneath a capping lid.

Strong (1986) and Smith and Yau (1993) described a conceptual model of severe convective outbreaks in Alberta as consisting of two stages. The first stage is characterized by a building upper level ridge which serves to cap deep convection in the foothills, although shallow convection supporting TCU or a small CB is possible. The second stage involves the breakdown of the upper level ridge with an upper level trough advancing from the west. Upper-level cooling, when combined with strong surface heating and the upslope transport of ample low-level moisture, commonly results in deep convection (Fig. 4). If the mid- and upper level winds are strong enough, the storm will advance eastward from the foothills affecting the more populated areas of Alberta.

2. Theoretical Overview

It is instructive to provide a brief description of environmental conditions conducive to supercell storm development to establish a context for the mesoscale analysis of later sections. Here we discuss the importance of drylines and differentiate between wind shear environments conducive to non-splitting and splitting supercells.

a. The Dryline

Drylines have been found to be associated with tornadic thunderstorms over southwestern Saskatchewan (Knott 1995, 1997) and over southern Alberta, the most famous example being the Edmonton tornado. A dryline is a narrow zone containing a sharp gradient of moisture in the planetary bounary layer (Shaw et al. 1997) separating distinctly dry and moist airmasses. It is often located within the warm sector of a frontal wave in a trough of low pressure or along a wind shift line. It is not considered a front in the classical sense, as temperatures in the dry air can be significantly higher in the daytime and lower during the nighttime hours than in the moist air ahead

of the dryline. Climatologically, drylines form in regions of sloping topography in which their orientation tends to parallel topographical contours (Schaefer 1986).

Drylines can be analyzed using surface observations of θ_e fields, mixing ratio, or dewpoint temperatures. Operationally, it is convenient to use measured dewpoint temperatures and satellite imagery to identify a dryline. Vertical soundings in the dry air typically display dry adiabatic lapse rates through the lower troposphere, often to 500 mb or higher (Schaefer 1986). Soundings in the moist air often exhibit a capping inversion around 800 mb to 700 mb with a well mixed layer above (Schaefer 1986). Consequently, a thunderstorm which manages to break the capping inversion in the moist air will develop in a high CAPE environment due to steep lapse rates in the dry mid-level air aloft.

Observational (e.g., Ziegler and Rasmussen 1998) and modeling studies (e.g., Ziegler et al. 1997) have investigated the role of drylines in the initiation of deep moist convection. Their findings concur with those of others, suggesting that the dryline is a thermally direct, solenoidally forced, frontogenetic secondary circulation (Ziegler et al. 1997). Differential heating and the resulting solenoidally driven upslope flow in the dryline environment generate horizontal convergence in the boundary layer thus frontogenetically increasing the horizontal gradients of temperature and moisture (Ziegler et al. 1997). The development of a narrow convergence line (and resulting ascent) along the dryline separating broad areas of subsidence, provides mesoscale lift within the boundary layer to initiate convection. The narrow updraft band is oriented with a component along the direction of boundary layer shear so that air parcels originating in the moist air are advected westward into the dryline updraft at low-levels and carried downstream (i.e., generally in a northward direction) during ascent. Once the LCL is reached, latent energy in the moist air enhances parcel buoyancy and, therefore, updraft velocity resulting in cumulus and / or towering cumulus development above the dryline. Environmental windshear across the dryline (i.e., west to east) tilts the trajectories of the moist ascending air to the east. As deeper convection develops in the absolutely unstable air above the boundary layer, mid-level wind shear and outflow boundary interactions cause the developing cells to propagate away from the dryline into the moist air where increased available latent energy promotes development of vigorous deep convection. The result is a flanking line of cumulus and towering cumulus over the dryline marking the inflow into a mature thunderstorm within a few 10's of km east of the dryline.

b. The supercell storm environment

The storm environment conducive to supercell development has unique characteristics. Given sufficient CAPE, the nature of the wind shear environment is crucial to mesocyclone development. Modeling studies (e.g., Wilhelmson and Klemp 1981; Weisman and Klemp 1986) have shown that curvature of the wind shear vector (hodograph) in the inflow layer of the storm is most important for the development of supercells. Generally, mesocyclone potential is high when the low-level winds are strong, the hodograph veers with height, and storm motion is well to the right of the environmental mean winds (Moller et al. 1994). Davies-Jones et al. (1990) suggest that the storm-relative winds in the lowest 3 km should be at least 10 ms^{-1} (36 kmh^{-1}) and should veer by at least 90° for mesocyclone development. Clockwise curvature of the wind shear vector leads to the development of perturbation pressure gradient forces favoring the right flank of the storm as a region for new development. The result is an upward directed pressure gradient force at low levels on the upwind side of the updraft (i.e., the region of storm inflow) and at upper levels in the storm above the inflow region (Davies-Jones 1985) thus enhancing vertical velocities.

Storm evolution is also dependent on the nature of the wind shear environment aloft. Numerical modeling studies indicate that continued clockwise curvature of the hodograph above the inflow layer favors a cyclonically rotating storm that propagates to the right of the mean environmental winds (Weisman and Klemp 1986). Unidirectional shear at higher levels, however, can lead to a pair of storms resulting from the split of an initial single thunderstorm cell.

c. The splitting supercell storm environment

In a unidirectionally sheared storm environment it is possible for an initial single thunderstorm cell to split into Left-Moving (LM) and Right-Moving (RM) members. When horizontal vorticity tubes are tilted into the vertical through updraft interactions, a mid-level vorticity couplet can result. The interaction of this couplet with the environmental wind shear leads to pressure perturbations that may or may not combine with a precipitation induced downdraft to induce storm splitting (Klemp 1987). For a rigorous examination of storm splitting theory, the reader is referred to Wilhelmson and Klemp (1981) and Klemp (1987).

Splitting storms have been documented both through numerical modeling experiments (e.g., Fujita and Grandoso 1968; Schlesinger 1980; Wilhelmson and Klemp 1981) and observationally (e.g., Achtemeier 1969; Bluestein and Sohl 1979; Bluestein and Woodall 1990). If the shear vector is unidirectional through most of the troposphere (straight hodograph) the result is a "mirror-image" pair of storms with the RM and LM storms rotating cyclonically and anti-cyclonically, respectively (Weisman and Klemp 1982, 1986). Theoretically, in such a case, neither storm is favored over the other and both persist (Moller et al. 1994).

An environment of clockwise hodograph curvature in the inflow layer accompanied by unidirectional shear aloft favours the development of a splitting storm where the RM storm may become supercellular and will be dominant over the LM storm (Weisman and Klemp 1986). While the LM storm may persist for some time, the RM storm is generally more intense and results in higher incidence of severe weather damage (e.g., from hail, winds, and tornadoes).

d. The radar observed storm-splitting process

The chief method of observing storm splitting is through radar observations. Case studies have shown that a common evolution of radar echoes exists both preceding and following a storm split. Brown and Meitín (1994) summarized the storm splitting process in four stages as follows:

1. Formation: A thunderstorm develops and moves to the east or northeast. A reflectivity gradient develops along its rear flank.

2. Elongation: The reflectivity structure elongates perpendicular to the mean wind and the central precipitation core maximum splits.

3. Splitting: The central reflectivity region splits leading to separate storm cells.

4. Deviation: The LM and RM storms deviate from the mean wind direction with their separation from one another increasing with time.

Recognition of the elongation of the central precipitation core accompanied by a reflectivity gradient along the storm's rear flank suggests to the severe weather meteorologist that splitting may be imminent.

3. Synoptic and Mesoscale Environment of 29 July 1993

a. Forecaster Situation Assessment

During the 24 hours preceding the severe weather outbreak of 29 July 1993, the upper air flow pattern revealed a high amplitude 500mb ridge over the Canadian Continental Divide with a 500mb low just west of Vancouver Island tracking slowly to the northeast at 5 knots. The 500mb ridge started to breakdown during the day on the 29th as the BC coast upper low accelerated and moved inland.

The breakdown of an upper ridge with a cold low advancing eastward from southern British Columbia has long been recognized as a pattern for severe convective weather over Alberta during the summer months. The Edmonton tornado (classified F4) of 31 July 1987 occurred with a similar a synoptic pattern. Consequently, on this day the severe weather forecaster had been expecting severe thunderstorms and was also contemplating a tornado watch for portions of Alberta later in the day. A severe thunderstorm watch was issued before noon (in accordance with office policy) for the regions northeast of Edmonton at Slave Lake, Fort McMurray and St Paul. This was considered the most likely threat area based on numerical guidance from the Canadian Regional Finite Element (RFE) model. The RFE forecast a developing westerly downslope surface wind over much of western and central portions of the province during the day with maximum surface convergence over northeastern Alberta. In addition, the placement of the upper level cooling behind the 850-500 mb thermal ridge was over northeastern Alberta as well.

As time progressed into the early afternoon hours it became increasingly apparent that the main area of concern would be considerably further southwest towards the foothills and the Red Deer/Edmonton areas. The surface temperatures/dewpoint and associated CAPE values were considerably higher than originally anticipated as the downslope surface westerly flow had failed to materialize as suggested by the RFE. Although the airmass was capped, there was a dryline developing near the foothills with significant moisture flux convergence ahead. The first severe weather report occurred late in the afternoon at 2245 UTC 80 km southwest of Edmonton prompting issuance of thunderstorm and tornado warnings shortly thereafter.

A surface analysis at 0000 UTC 30 July revealed a low pressure center just west of Edmonton and a thermal low 50 km to the northeast of Edmonton. A warm front extended northeastwards to Cold Lake while a quasi-stationary front extended southwards from the low to another frontal wave near Red Deer. An eastward moving cold front extended southeastwards from the Red Deer wave to Brooks. Within the warm sector there was a south-southeasterly 30 knot low-level jet over Saskatchewan and a moisture axis extending from Regina to Edmonton. The surface dewpoint temperatures in the warm sector were quite high for Alberta with values in the 18°C to 21°C range resulting in CAPE values from 2000 Jkg^{-1} to 3500 Jkg^{-1} (Archibald 1993).

The corresponding upper level features revealed a 250 mb 130 knot southerly jet core over Idaho. A 500 mb south-southwesterly flow of 40 to 60 knots was present over central Alberta while a 40 knot flow of air at 700 mb streamed southwesterly over southern Alberta. The 1000-500 mb thickness ridge, and the 700 mb thermal ridge, had advanced into the warm sector allowing for

destabilization ahead of and parallel to the analyzed cold front and dryline. Figure 5 is a composite map illustrating the major features from 0000 UTC.

In summary, the greatest convective forcing and instability resided in the more classic area of the Alberta foothills near Red Deer. The RFE model data suggested that severe weather would occur further northeast than was observed. It was too fast in pulling the lee trough from the foothills, consequently the westerly downslope flow which was forecast over the Edmonton/Red Deer areas did not occur and was rather replaced by warm moist air, a light southeasterly flow and moderately high CAPE values. In addition, the surface dewpoint temperature gradient was poorly resolved. Although general drying was forecast from west to east the RFE dewpoint temperatures were approximately 5°C too dry in the moist air and 8°C too moist in the dry air. Thus the modeling of the boundary layer to the lee of the Canadian Rockies was not well handled and the severe weather forecaster had to adapt his original thinking and concentrate on a more populated area further to the southwest.

b. Dryline

During the morning hours of the 29th there was no evidence of a pronounced dewpoint temperature gradient or dryline over Alberta. As the day evolved, a southeasterly flow from the Dakota States and eastern Montana produced an axis of dewpoint maxima from Regina to Edmonton with values of 18°C to 21°C. The strong upper-level southwesterly flow originating from the higher terrain of British Columbia and the northwestern United States produced strong subsidence in the lee of the Rockies forming a dryline. Passage of the dryline was strongly correlated with a fall in surface dewpoint temperature and a shift in the surface wind direction from southeasterly to southwesterly. The initial transition to significantly drier air was observed in the Calgary area at 2000 UTC. The wind veered from southeasterly to southerly at this time before ultimately prevailing from the southwest for the remainder of the evening. The dewpoint temperature fell 9.6°C in two hours. Sundre, located 90 km north-northwest of Calgary, also experienced substantially drier air moving in from the southwest at 2000 UTC. Dryline passage at Red Deer and Coronation occurred near 0100 UTC and 0200 UTC respectively. The temporal evolution of surface dewpoint temperature and wind direction at Calgary, Sundre, and Red Deer is summarized in Figure 6.

The location of the dryline was analyzed as being on the leading edge of strong dry air advection. The dryline location relative to the frontal analysis was atypical of that described in the literature in that it did not neatly drop southward in the warm sector from the low center. Rather, it was more closely associated with the analyzed surface and 850 mb cold front (see Fig. 5). The 0000 UTC dryline location indicated a bulging of the dryline near Coronation (Fig. 7). Schaefer (1986) states that thunderstorms are most likely to form along the portion of the bulge that is oriented from northwest to southeast. This configuration tends to maximize convergence as winds in the moist air "wrap" around the dry air. This appeared to be the case on 29 July as two supercell thunderstorms developed near this portion of the dryline.

c. Sounding analysis

Our interest in the operational aspects of the severe weather outbreak prompted us to choose the 1200 UTC sounding to describe the mesoscale upper air environment. During the morning convective assessment this is the only observational sounding data available for Alberta. Modification of the 1200 UTC sounding with surface observations obtained closer to the time of

storm development simulates the data available to the forecaster. While the 0000 UTC sounding may be more representative of the pre-storm environment, convection in Alberta is typically underway by the time the 0000 UTC sounding becomes available.

The 1200 UTC 29 July 1993 Stony Plain (53.55°N, 114.10°W) sounding (Fig. 8) shows a capping inversion (negative buoyant energy of 58 Jkg^{-1}) up to 800 mb with an unstable (nearly dry adiabatic) temperature profile aloft. The 700 mb to 500 mb temperature difference (ΔT_{75}) was 21°C. Alberta forecasters generally consider ΔT_{75} in excess of 20°C to be indicative of the potential for deep convection in the central Alberta region. The 1200 UTC surface temperature and dewpoint at Stony Plain were 15.0°C and 13.9°C, respectively. Both would rise throughout the day prior to initiation of convection reaching values of 26°C and 17°C, respectively, in Red Deer at 2300 UTC (2 hours prior to development of the Holden storm and before the passage of the dryline). The moisture profile shows relatively dry air above the inversion with a relative humidity at 700 mb of only 39%. This capping of dry air, exhibiting a steep lapse rate, over warm, moist low-level air is characteristic of the classic loaded gun sounding. Using the Red Deer temperature and dewpoint from surface observations at 2300 UTC, CAPE is 2896 Jkg^{-1}.

The hodograph from the 1200 UTC Stony Plain sounding (Fig. 9) shows veering of the winds in the lowest kilometer with slight backing between ~1 km and 2 km. The hodograph then indicates strong, approximately unidirectional wind shear above 3km up to 200 mb (~11 km) where the winds were from the southwest at nearly 35 ms^{-1} (68 kt). The hodograph also shows veering of the storm-relative winds in excess of 90° with speeds near 10 ms^{-1} meeting the mesocyclone development criteria of Davies-Jones et al. (1990). The surface to 6 km mean wind shear was calculated to be $6.8x10^{-3}$ s^{-1} and the surface to 4 km mean wind shear to be $8.3\ x10^{-3}$ s^{-1}. Weisman and Klemp (1982) found surface to 6 km mean shear values of around $6\ x10^{-3}$ s^{-1} were associated with numerically modeled splitting storms. Rasmussen and Wilhelmson (1983) plotted storm occurrence from 13 cases as a function of CAPE and 0-4 km mean wind shear. Comparing our values of CAPE and wind shear with the their results, we find the modified 1200 UTC 29 July sounding to lie in the region associated with multiple tornado case days.

Using the unmodified hodograph at 12Z the surface to 3km Storm Relative Helicity (SRH) was calculated to be $44m^2s^{-2}$ using a theoretical storm motion (e.g., Maddox 1976) of $10ms^{-1}$ from 239° and $40m^2s^{-2}$ using the radar observed motion of the RM Holden storm of $12ms^{-1}$ from 230°. These values of SRH are low suggesting that, in light of the confirmed multiple tornadoes on the 29th, the wind environment prior to and during storm development was different from that observed from the 1200 UTC sounding and likely had higher SRH values associated with it. Using surface winds and model data on this day, Archibald (1993) calculated SRH to be < 100 m^2s^{-2} in the Holden area but nearly 300 m^2s^{-2} at Lloydminster during the time the storms were active.

The bulk Richardson number from the modified 1200 UTC sounding is 30. This is within the range of ~10 to 50 suggested for supercell storms and also within the range for splitting storms of ~15 to 45 (Weisman and Klemp 1982). Combining the CAPE and SRH values into the Energy-Helicity Index we find an EHI of 1.0. EHI values ≥1 are generally indicative of the potential for tornado development (Brooks et al. 1994).

In summary, the 1200 UTC sounding indicates the mesoscale environment was characterized by large CAPE, strong mean wind shear, relatively low SRH and approximately unidirectional wind shear above 3 km. Unidirectional wind shear above the lowest three kilometers should prompt the

forecaster to also consider the development of splitting severe storms. Anticipation of storm splitting could allow more accurate and timely issuance of severe weather warnings to areas that may otherwise go unaffected by the developing storms.

It is interesting to note that in this case, the proximity of the low pressure center to Stony Plain meant that the 0000 UTC sounding was not in the warm sector of the wave and therefore was likely not representative of the storm environment. The wind profile from the 0000 UTC sounding (not shown) indicated significant cold air advection in the lowest few kilometers and the surface winds in the Stony Plain area were northwesterly from 2000 UTC onwards. The resulting SRH was negative. The thermodynamics are not significantly different from the 1200 UTC sounding with CAPE values ~3000 Jkg^{-1} using the same surface observations as were used to modify the 1200 UTC sounding.

4. Observational Analysis

a. Radar observed storm evolution

Analysis of radar imagery revealed nearly parallel storm tracks as illustrated in Fig. 10. Only long track, severe storms attaining a >52 dBZ core are shown from analysis of the Carvel Doppler radar (located 40 km west of Edmonton) 1.5 km CAPPI imagery. Each storm is labeled alphabetically in chronological order. The severe weather events reported that correspond to each storm are summarized in Table 1.

The Pigeon Lake storm (storm A) developed at 2130 UTC near Rocky Mountain House within 30 km of the dryline. The cell did not develop a 52 dBZ core until 2210 UTC. This storm moved to the northeast at an average speed of ~52 kmh^{-1} with a total track length of 209 km. At the earliest stages of this storms development it appears as though the central precipitation core may have split (~2200 UTC) with the RM storm becoming the Pigeon Lake storm. The LM storm had a >52 dBZ echo core for only 20 min before the cell dissipated. This storm did not show the characteristic features of splitting storms outlined in section 2*c* and as no intense precipitation core was observed prior to 2210 UTC it is not clear whether the short lived LM storm resulted from a split of the original storm or merely from new development on the left flank of the parent storm. There were reports of baseball hail at 2245 UTC and golfball hail at 2330 UTC associated with the Pigeon Lake storm. This cell also produced a tornado at Falun, near Pigeon Lake, around 0000 UTC. Radar imagery indicated that the storm had a kidney bean shape for most of its life with an occasional marked pendant echo on the south flank. The severe storm map radar product[1] (Crozier et al. 1991) measured the height of the 40 dBZ returns to be in excess of 12 km from 2220 UTC until 0040 UTC indicative of a strong sustained updraft. In addition, Doppler radial velocities revealed strong convergence on the inflow side of the storm with rotation observable on the 0.5° PPI and 3.5° PPI preceding and at the time of the F0 tornado report. The storm dissipated shortly after 0140 UTC approximately 60 km northeast of the city of Edmonton.

The Holden storm (storm B) developed around 0100 UTC just northwest of Red Deer and within 10 km of the analyzed dryline location. It tracked away from the dryline on a parallel track to storm A. Approximately one hour into its evolution this storm began its splitting process elongating

[1] The severe storm map product, developed by the King City radar group, measures the height AGL of the 40 dBZ reflectivity.

along an axis perpendicular to cell motion between Camrose and Wetaskiwin before ultimately splitting into distinct cells just north of Camrose. The right deviating cell produced a damaging F3 tornado in the Holden area. The Holden storm will be discussed in greater detail in section 4*b*.

The Edmonton storm (storm C) formation process was different from the first two cells described. A cluster of convective cells 120 km west of Edmonton produced a large outflow boundary detected on Doppler radar. The portion of the boundary measured by Doppler was at least 115 km in length, approximately 1.0 km in height, and traveled eastwards 85 km through stable, rain-cooled air at a speed of 60 kmh^{-1} before triggering a convective cell right over the city of Edmonton. Archibald (1993) described this boundary as the cold front. It is indeed likely that this boundary provided the final eastward push of the warm sector which was lingering in the Edmonton area. This storm produced golf ball hail, strong winds and local flooding in the southeastern Edmonton area at midnight (0600 UTC). The cell then tracked northeastwards at 75 kmh^{-1} producing damaging straight line winds (damage to motel, granary, road signs and trees down) at 0725 UTC over Smoky Lake (Vickers 1993). From the severe storm map, it is apparent that this cell had the weakest updraft of the severe storms observed on the 29th. Over Edmonton, portions of the cell had 40 dBZ between 8.5 km and 10.5 km, a height that Alberta severe weather forecasters generally associate with borderline severe storms, and by the time the cell reached Smoky Lake a height of only 5.5 km to 8.5 km was observed. The low level CAPPI imagery near Smoky Lake revealed a bow echo structure (0720 UTC) which was consistent with the location of straight line wind damage in the area.

The Lac la Biche storm (storm D) formed at roughly the same time as the Edmonton storm although the gust front believed to have triggered it appeared to be 20 km to the west. This storm formed northeast of Edmonton and split in to LM and RM members at around 0620 UTC. The splitting process described previously was observed to some degree in this storm as the central precipitation core elongated perpendicular to the direction of storm motion prior to the split. The RM storm produced a tornado in the Lac La Biche area (150 km northeast of Edmonton) as well as measured winds of 144 kmh^{-1} at an Alberta Forestry tower at around 0800 UTC. The height of the 40 dBZ echoes were between 10.5 km and 12.0 km, indicative of a strong updraft. While this storm tracked mostly through sparsely populated areas, the heights of the 40 dBZ returns suggest that large hail could also have been produced.

b. The Holden storm

The Holden storm first appeared on radar at 0020 UTC with a reflectivity of 42 dBZ. By 0100 UTC the storm had a >52 dBZ core and was tracking northeast at ~54 kmh^{-1}. By this time the storm already had a strong reflectivity gradient on its right flank indicative of the inflow region. The storm continued to grow and the core elongated on an axis perpendicular to its direction of motion around 0230 UTC. A marked reflectivity gradient along the rear flank was evident at this time. By 0300 UTC the storm had split into LM and RM cells that continued to separate with the LM and RM storms propagating at 61 kmh^{-1} and 43 kmh^{-1} respectively. The speed of propagation of the LM and RM storms is consistent with results summarized by Brown and Meitín with the LM storm consistently propagating faster than the RM storm.

Following the initial storm split at 0300 UTC, the LM storm subsequently split around 0320 UTC. The characteristic storm splitting features discussed in section 2b were again apparent during this second split. Elongation of the precipitation core of the LM storm occurred between 0250 UTC and 0310 UTC with a strong reflectivity gradient on the rear flank prior to splitting. The new left-

moving storm (LM_2) was weak with a >52 dBZ precipitation core only until 0330 UTC and briefly again at 0420 UTC. The new right-moving storm (RM_2) persisted well after dissipation of the initial RM storm with 40 dBZ returns above 10.5 km intermittently until 0440 UTC and storm tops higher than 14 km until 0550 UTC. Similar cases of multiple storm splits have appeared in the literature (e.g., Wilhelmson and Klemp 1981). The RM_2 storm developed a reflectivity gradient on its right flank following the second split but did not deviate to the right of the mean wind to the same extent as the RM storm. While there were no reports of severe weather events with the RM_2 storm, the 1.5 km CAPPI and severe storm composite products indicate that this storm quite probably produced severe hail (i.e., ≥ 20 mm in diameter). The splitting process of the Holden storm is illustrated in Fig. 11 with each of the four splitting stages indicated. The process is also summarized in Table 2.

The 1.5 km CAPPI image at 0300 UTC shows a distinct hook echo on the right flank of the RM storm consistent with a Weak Echo Region (WER) and strong storm inflow. The echo tops and severe storm maps at this time show storm tops in excess of 14 km and the height of the 40 dBZ return to be higher than 12 km directly over the WER indicative of a strong, organized storm updraft. The LM storm at this time had a storm top in excess of 14 km but the height of the 40 dBZ return was only 8.5 km to 10.5 km AGL illustrating the increased intensity of the RM storm.

The most pronounced hook echo associated with the RM storm occurred prior to the Holden tornado from 0300 UTC to 0340 UTC. Golfball sized hail was reported in Camrose at 0250 UTC and in Ryley at 0340 UTC. Fig. 12 shows contours of the 1.5 km CAPPI with heights of the 40 dBZ reflectivity superimposed (dashed lines). The "overhang" of strong reflectivity and storm top over the WER clearly indicates the presence of a strong updraft within a well organized storm and is consistent with the reflectivity structure typical of a classic supercell (Lemon and Doswell 1979; Moller et al. 1994). During most of the time the tornado was on the ground the height of the 40 dBZ reflectivity was in excess of 12 km. The tornado associated with this storm was reported on the ground around 0340 UTC just west of the town of Holden and is thought to have been on the ground between 0340 and 0400 UTC. The radar image at 0340 UTC was likely very near the time of tornado development. The likely position of the tornado within the hook echo region was approximately 8 km west of Holden at 0340 UTC. By 0350 UTC the likely location of the tornado was very near the town itself. Curiously, there is a rapid decrease in storm strength from 0330 UTC to 0410 UTC, or during the time of the tornado. By 0400 UTC the RM storm had lost its distinct hook echo but still maintained a kidney shaped reflectivity pattern until its dissipation near 0430 UTC. Unfortunately, the thunderstorm was beyond 120 km from Carvel radar thus no radial velocity imagery could be measured for this storm.

A damage survey in the Holden area (Vickers and Kochtubajda 1993) suggests that an F3 tornado was on the ground for approximately 20 minutes between 0340 and 0400 UTC. The estimated path length was 16-17 km located just west of the town of Holden from southwest to northeast. The path width was initially ~100 m increasing to 250 m at its widest point. While the tornado did track through a relatively sparsely populated area, two people were injured as the tornado flipped several mobile homes. The tornado also twisted and snapped trees, wrapped corrugated sheet metal around trees, caused irreparable damage to a large brick and mortar building and destroyed well constructed farm buildings in its path.

5. Summary and Conclusions

On 29 July 1993 central Alberta was subjected to a significant severe weather outbreak. Warm temperatures, high dewpoint temperatures, and upper level cooling moving across the mountains from the west combined to generate conditions conducive to severe thunderstorms. A dryline originating in the southwest corner of the province helped trigger the convection. CAPE values on this day ranged from 2000 Jkg^{-1} to 3500 Jkg^{-1} and the storms developed in an environment of strong unidirectional mid-level shear. Three tornadoes were reported, one of F3 strength, as were large hail and damaging winds. The most severe storms followed nearly parallel tracks from southwest to northeast at speeds ranging from ~50 to 75 kmh^{-1}.

There were a number of features associated with this storm outbreak that are interesting from an operational perspective. The first is the presence of a dryline that first appeared at Calgary and Sundre at 2000 UTC and proceeded to move from the foothills eastwards and northeastwards. Dewpoint temperature falls of 6°C to 10°C in 2 hours were observed at numerous sites and were found to correlate well with veering of the surface winds from southeasterly to southwesterly. The first two strong thunderstorms on the 29th, including the one that produced the Holden tornado, developed northeast and within 30 km of the dryline. This dryline likely played a role in the initiation and environment of these storms. It is important for the severe weather forecaster to recognize the signs of dryline formation to identify areas of potential severe thunderstorm development. This is especially true with drylines that may bulge eastward due to the mixing down of dry air associated with a strong mid-level jet streaming over the Rockies. The enhanced low-level convergence northeast of the dryline bulge increases the probablility of convection being triggered. This is the fourth documented case in the past 12 years which involved a well defined dryline and a significant tornado outbreak over the southwestern Canadian plains. Other dates include 29 August 1995 over southern Saskatchewan, 28-29 June 1993 southwestern Saskatchewan and 31 July 1987 over central Alberta.

Secondly, the 1200 UTC Stony Plain sounding indicated a wind shear environment conducive to splitting severe storms as discussed by Wilhelmson and Klemp (1981) and Weisman and Klemp (1986). The hodograph showed some veering of the winds at low levels with strong, relatively unidirectional wind shear aloft. This type of hodograph favours splitting storms with dominant RM members as was observed with the Holden storm, the Lac la Biche storm, and possibly the Pigeon Lake storm. Thirdly, the storms that did split exhibited radar observed features that have been found to be characteristic of splitting storms. The Holden storm developed a reflectivity gradient on its rear flank and the central precipitation core elongated perpendicular to the direction of storm motion prior to splitting. A similar process preceded the second split of the LM storm. Recognition of radar observed characteristics associated with storm splitting allows the forecaster to nowcast the splitting before it happens.

Lastly, the Edmonton storm that developed around 0600 UTC was triggered by an outflow boundary that traveled 85km from the West. The outflow boundary was generated by an area of convection in the Edson and Swan Hills area. It did not trigger any significant convection until it reached an area of warm unstable air residing in the Edmonton area and within 40 km east.

While conducting post event studies allows in depth examination of features associated with the event, the forecaster can be aware of impending events if their warning signs are heeded. On days when deep convection is expected, hints of dryline development prior to thunderstorm development can indicate an increased potential for strong (possibly tornadic) convection as well as providing a

boundary along which storm initiation may occur. In an environment of large CAPE and strong unidirectional shear of the winds aloft, the conditions may be ideal for splitting severe storms. On 29 July 1993, the possible split of the Pigeon lake storm suggested that splitting of future storms should be considered. While observing the Holden and Lac la Biche storms, the elongation of the central precipitation core and reflectivity gradient along the rear flank suggested that splitting was imminent. Knowing this, the forecaster could expect that two storms deviating to the right and left of the mean winds was a likely result and could adjust the thunderstorm warning areas accordingly. Lastly, while outflow boundary interactions between storms is a well known trigger for convection, even gust fronts propagating in rain cooled air can travel long distances to initiate convection in more unstable air masses in their path.

While in the "heat of the battle" the forecaster cannot observe every mesoscale nuance, the authors feel that correct diagnosis and prognosis of such processes as dryline formation and storm splitting allow the severe weather meteorologist to anticipate and quickly adapt severe thunderstorm and tornado warning areas to the benefit of the general public.

Acknowledgments

The authors wish to thank Dr. Gerhard Reuter of the University of Alberta for provision of radar data. In addition, the author's appreciate the comments and support of the staff at the Prairie Aviation and Arctic Weather Center (PAAWC) of Environment Canada, in particular Glenn Vickers, Jamie Archibald, Steve Ricketts and Brian Paruk.

Authors Page

Stephen Knott is program manager of Science and Training with the Prairie Aviation and Arctic Weather Center of the Meteorological Service of Canada. He received a B.Sc. in meteorology from McGill University in 1984 and joined Environment Canada in 1985 as an operational meteorologist. He became a Training Branch Instructor for the Meteorologist Operations Course (MOC) in Toronto from 1987 to 1992. Other assignments included a one year posting at King City Radar, five years as severe weather program manager for the Saskatchewan Environmental Services Centre in Saskatoon and two years as a severe weather meteorologist for the Prairie Storm Prediction Centre - Edmonton unit.

Neil Taylor is an aviation forecaster with the Prairie Aviation and Arctic Weather Center of the Meteorological Service of Canada. Following a B.Sc. in Physics with specialization in Astrophysics from the University of Waterloo, Neil received his M.Sc. in Meteorology from the University of Alberta. His thesis involved compiling a climatology of convective sounding parameters for central Alberta and investigating parameter thresholds associated with severe thunderstorm development in the region.

References

Achtemeier, G. L., 1969: Some observations of splitting thunderstorms over Iowa on August 25-26, 1965. Preprints, *6th Conference on Severe Local Storms.* Chicago, Amer. Meteor. Soc., 89-94.

Archibald, J. 1993: An Analysis of the Severe Weather Outbreak in Central Alberta 29 July 1993, *Tech. Memo,* Environment Canada.

Bluestein, H. B. and C. J. Sohl, 1979: Some observations of a splitting severe thunderstorm. *Mon. Wea. Rev.*, **107**, 861-878.

Bluestein, H. B., and G. R. Woodall, 1990: Doppler-radar analysis of a low-precipitation severe storm. *Mon. Wea. Rev.*, **118**, 1640-1664.

Brooks, H. E., C. A. Doswell III, and J. Cooper, 1994: On the environments of tornadic and non-tornadic mesocyclones. *Wea. Forecasting*, **9**, 606-618.

Brown, R. A. and R. J. Meitin, 1994: Evolution and morphology of two splitting thunderstorms with dominant left-moving members. *Mon. Wea. Rev.*, **122**, 2052-2067.

Bullas, J. M. and A. F. Wallace, 1988: The Edmonton tornado, July 31, 1987. Preprints, *15th Conf. on Severe Local Storms*, Baltimore, Maryland, Amer. Meteor. Soc., 437-443.

Chisholm, A. J., 1973: Alberta Hailstorms. Part I: Radar case studies and airflow models. *Meteor. Monogr.*, No. 36, Amer. Meteor. Soc., 1-36.

Chisholm, A. J. and J. H. Renick, 1972: The kinematics of multi-cell and supercell Alberta hailstorms. Alberta Hail Studies 1972. Alberta Research Council, Edmonton, Alberta, Hail Studies Report 72-2, 24-31.

Crozier, C.L., P. I. Joe, J.W. Scott, H.N. Herscovitch and T.R. Nichols, 1991: The King City operational Doppler radar: development, all season applications and forecasting, *Atmos. Ocean*, **29**, 479-516.

Davies-Jones, R., 1985: Dynamical interaction between an isolated convective cell and a veering environmental wind. Preprints, *14th Conf. on Severe Local Storms*, Indianapolis, Indiana, Amer. Meteor. Soc., 216-219.

Davies-Jones, R. P., D. Burgess, and M. Foster, 1990: Test of helicity as a tornado forecast parameter. Preprints, *16th Conf. on Severe Local Storms*, Kananaskis Park, Alberta, Amer. Meteor. Soc., 588-592.

Fujita, T., and H. Grandoso, 1968: Split of a thunderstorm into anticyclonic and cyclonic storms and their motion as determined from numerical model experiments. *J. Atmos. Sci.*, **25**, 416-439.

Klemp, J. B., 1987: Dynamics of Tornadic Thunderstorms. *Annu. Rev. Fluid Mech.*, **19**, 369-

402.

Knott, S.R.J. and D. E. Dudley, 1995: Saskatchewan Dryline Episode: 28-29 June 1994. Tech. Note. Prairie and Northern Region, Environment Canada.

Knott, S.R.J., 1997: Dry Line Analysis of the Spring Valley Tornado Event: 29 August 1995, Tech. Note. Prairie and Northern region, Environment Canada.

Kozak, S. A., 1998: Lightning strikes in Alberta thunderstorms: Climatology and case studies. M.Sc. Thesis, Department of Earth and Atmospheric Sciences, University of Alberta, 129 pp.

Lemon, L. R., and C. A. Doswell III,1979: Severe thunderstorm evolution and mesocyclone structure as related to tornadogenesis. *Mon. Wea. Rev.*, **107**, 1184-1197.

Longley, R. W. and C. E. Thompson, 1965: A study of the causes of hail. *J. Appl. Meteor*., **4**, 69-82.

Maddox, R. A., 1976: An evaluation of tornado proximity wind and stability data. *Mon. Wea. Rev.*, **104**, 133-142.

McCarthy, J. and S. E. Koch, 1982: The Evolution of an Oklahoma Dryline. Part 1: A Meso- and Synoptic-Scale Analysis, *J. Atmos. Sci.*, **39**,225-236.

McCarthy, P: 1998: A note on the average number of severe weather events for the prairies. *Personal communication*.

Moller, A. R., C. A. Doswell III, M. P. Foster, and G. R. Woodall, 1994: The operational recognition of supercell thunderstorm environments and storm structures. *Wea. Forecasting*, **9**, 327-347.

Newark, M. J., 1984: Canadian Tornadoes, 1950-1979. *Atmos. Ocean*, **22**, 343-353.

Paruk, B. J. and S. R. Blackwell, 1994: A severe thunderstorm climatology for Alberta. *National Weather Digest*, **19**, 27-33.

Rasmussen, E. N., and R. B. Wilhelmson, 1983: Relationships between storm characteristics and 1200 GMT hodographs, low-level shear, and stability. Preprints, *13th Conf. on severe local storms*, Amer. Meteor. Soc., J5-J8.

Schaefer, J. T., 1986: The Dryline. *Mesoscale Meteorology and Forecasting*, P. S. Ray, Ed., Amer. Meteor. Soc., 549-572.

Schlesinger, R. E., 1980: A three-dimensional numerical model of an isolated deep thunderstorm. Part II: Dynamics of updraft splitting and mesovortex couplet evolution. *J. Atmos. Sci.*, **37**, 395-420.

Shaw, B.L., Pielke, R.A., and C.L., Ziegler, 1997: A three-dimensional numerical simulation of a

great plains dryline. *Mon. Wea. Rev.*, **125**, 1489-1506.

Smith, S. B. and M. K. Yau, 1993a: The causes of severe convective outbreaks in Alberta. Part I: A comparison of a severe outbreak with two non-severe events. *Mon. Wea. Rev.*, **109**, 1099-1125.

Smith, S. B. and M. K. Yau, 1993b: The causes of severe convective outbreaks in Alberta. Part II: Conceptual model and statistical analysis. *Mon. Wea. Rev.*, **109**, 1126-1133.

Smith, S. B., G. W. Reuter, and M. K. Yau, 1998: The episodic occurrence of hail in central Alberta and the Highveld of South Africa. *Atmos. Ocean.*, **36**, 169-178.

Strong, G. S., 1986: Synoptic to mesoscale dynamics of severe thunderstorm environements: A diagnostic study with forecasting implications. Ph.D. Thesis, Department of Geography, University of Alberta, 345 pp.

Vickers, G. and Kochtubadja B. 1993: Damage survey near Holden and Smoky Lake, 29 July 1993. Northern Alberta Environmental Services Centre, Environment Canada.

Vickers, G, 1994: 1993 summer severe weather report for central and northern Alberta. Northern Alberta Environmental Services Centre, Environment Canada.

Weisman, M. L., and J. B. Klemp, 1982: The dependence of numerically simulated convective storms on vertical wind shear and buoyancy. *Mon. Wea. Rev.*, **110**, 504-520.

Weisman, M. L. and J. B. Klemp, 1986: Characteristics of isolated storms. *Mesoscale Meteorology and Forecasting*, P. S. Ray, Ed., Amer. Meteor. Soc., 331-357.

Wilhelmson, R. B. and J. B. Klemp, 1981: A three dimensional numerical simulation of splitting severe storms on 3 April 1964. *J. Atmos. Sci*., **38**, 1581-1600.

Wojtiw, L., 1975: Climatic summaries of hailfall in central Alberta (1957-1073). Alberta Research Council, Edmonton, Alberta, Atmos. Sci. Rep. 75-1, 102 pp.

Ziegler, C. L., T. J. Lee, and R. A. Pielke Sr., 1997: Convective initiation at the dryline: A modeling study. *Mon. Wea. Rev.*, **125**, 1001–1026.

Ziegler, C. L. and E. N. Rasmussen, 1998: The initiation of moist convection at the dryline: Forecasting issues from a case study perspective. *Wea. Forecasting*, **13**, 1106–1131.

List of Figures

Figure 1: Climatological distribution of severe thunderstorm events (1982 to 1991) per year per 10 000 square kilometers (from Paruk and Blackwell 1993, used by permission of author).

Figure 2: Average lightning strike density in Alberta for the summer months (June, July, and August) over the twelve year period 1984 to 1995 (adapted from Kozak 1998).

Figure 3: Climatological dewpoint temperature (°C) for July for the prairie provinces (adapted from Smith and Yau 1993).

Figure 4: Schematic diagram of the mountain - plain circulation as described by Smith and Yau (1993) showing moist air "under-running" the capping lid and convection beginning over the foothills (adapted from Smith and Yau 1993).

Figure 5: Composite figure at 0000 UTC 30 July 1993 showing the jet cores at 500mb, 700mb, and 850mb (arrows), the 500mb trof (double dashed line), and the 700mb thermal axis (dotted line). The location of the surface dryline, dewpoint temperature axis and fronts are indicated by the conventional symbols.

Figure 6: Temporal evolution of dewpoint temperature and wind direction for Calgary (YYC), Sundre (WAV), and Red Deer (YQF). Observations missing for WAV at 0100 UTC and dewpoint temperatures are below 0°C at 2100 UTC and 0200 UTC.

Figure 7: Alberta dryline evolution depicted by isochrones in 2 hour increments from 2000 UTC until 0200 UTC.

Figure 8: Skew-T Log P diagram from the 1200 UTC 29 July 1993 Stony Plain sounding using modified surface temperature and dewpoint of 26.2°C and 17.0°C, respectively. Buoyant energy is shaded and the wind profile is illustrated at right in knots.

Figure 9: Unmodified hodograph for 1200 UTC 29 July 1993. Heights are in metres AGL.

Figure 10: Composite storm tracks for 29-30 July 1993. The >52 dBZ core is contoured in 30 min intervals with all times in UTC. The storm tracks are labeled A, B, C, D corresponding to the Pigeon Lake, Holden, Edmonton, and Lac La Biche storms, respectively. The severe weather event markers are given in the upper left corner and the events are labeled as in Table 2.

Figure 11: Storm tracks for the Holden splitting storm. The contours correspond to dBZ reflectivity values of 42 dBZ and ≥ 52 dBZ. The storm is contoured at 30 min intervals with all times in UTC.

Figure 12: Composite radar image of the Holden storm at 0340Z (the approximate time the tornado was first sighted) showing 1.5km CAPPI reflectivities of 28 dBZ (lightly stippled), 42 dBZ (moderately stippled), and ≥ 52 dBZ (heavily stippled) and contoured heights of the 40 dBZ reflectivity (dashed) at 8.5km, 10.5km and ≥12km intervals. The approximate location of the storm top is indicated by a dot directly above the WER.

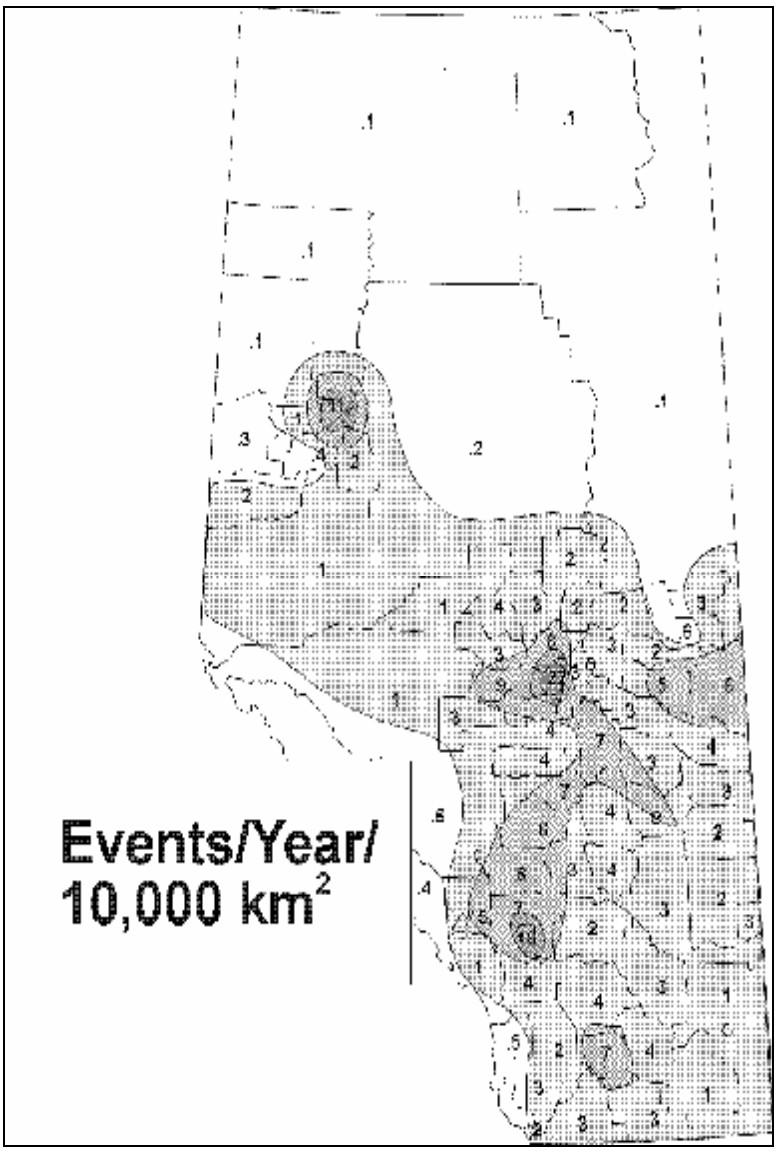

Figure 1: Climatological distribution of severe thunderstorm events (1982 to 1991) per year per 10 000 square kilometers (from Paruk and Blackwell 1993, used by permission of author).

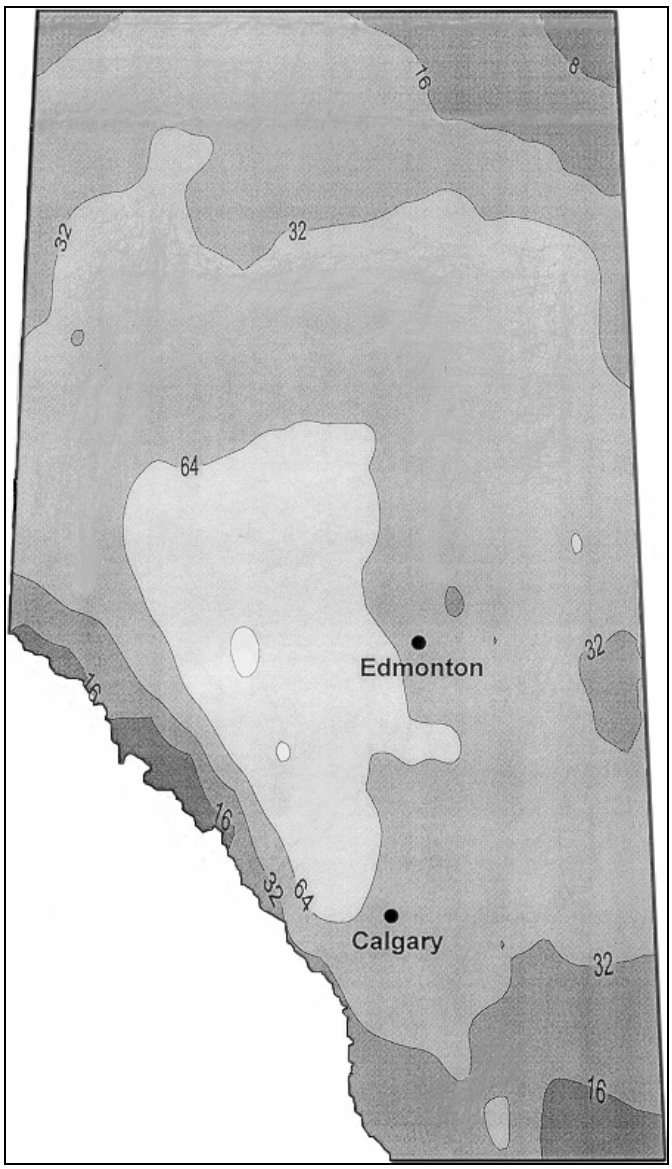

Figure 2: Average lightning strike density (per 10 km^2) in Alberta for the summer months (June, July, and August) over the twelve year period 1984 to 1995 (adapted from Kozak 1998).

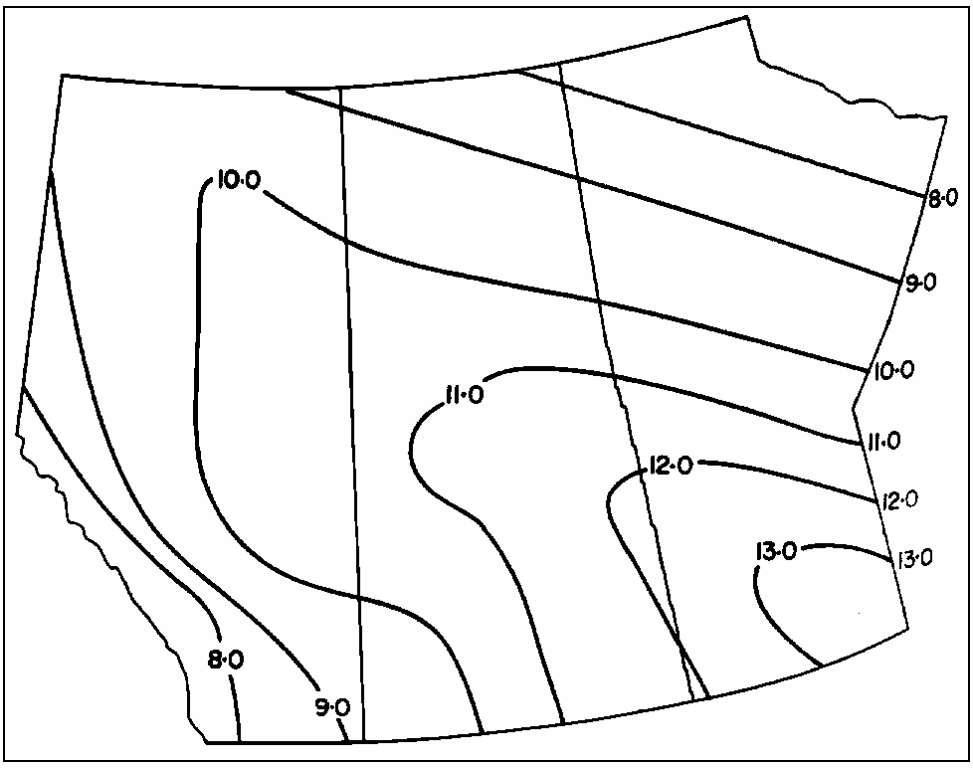

Figure 3: Climatological dewpoint temperature (°C) for July for the prairie provinces (adapted from Smith and Yau 1993).

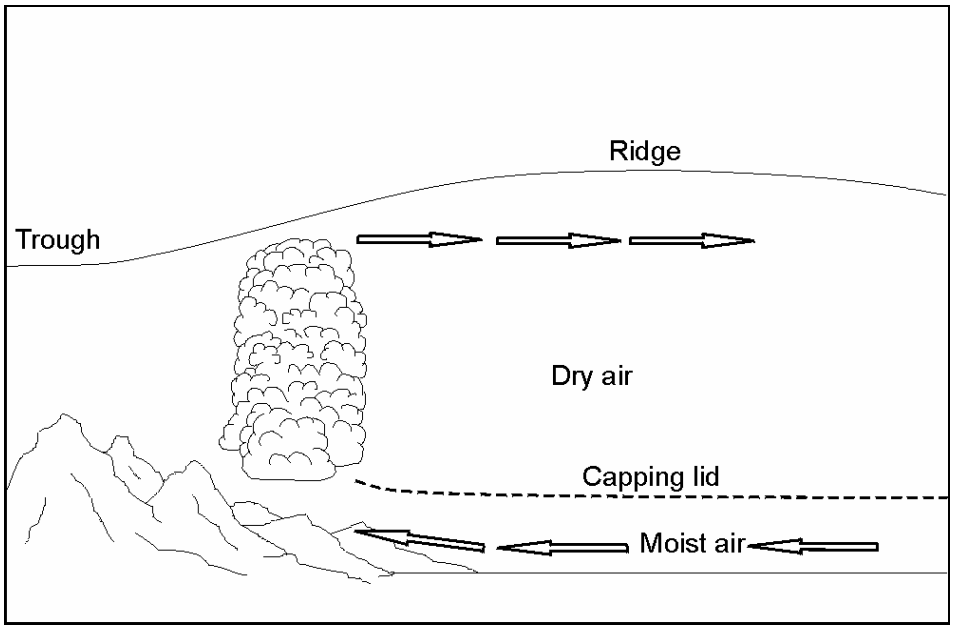

Figure 4: Schematic diagram of the mountain - plain circulation as described by Smith and Yau (1993) showing moist air "under-running" the capping lid and convection beginning over the foothills (adapted from Smith and Yau 1993).

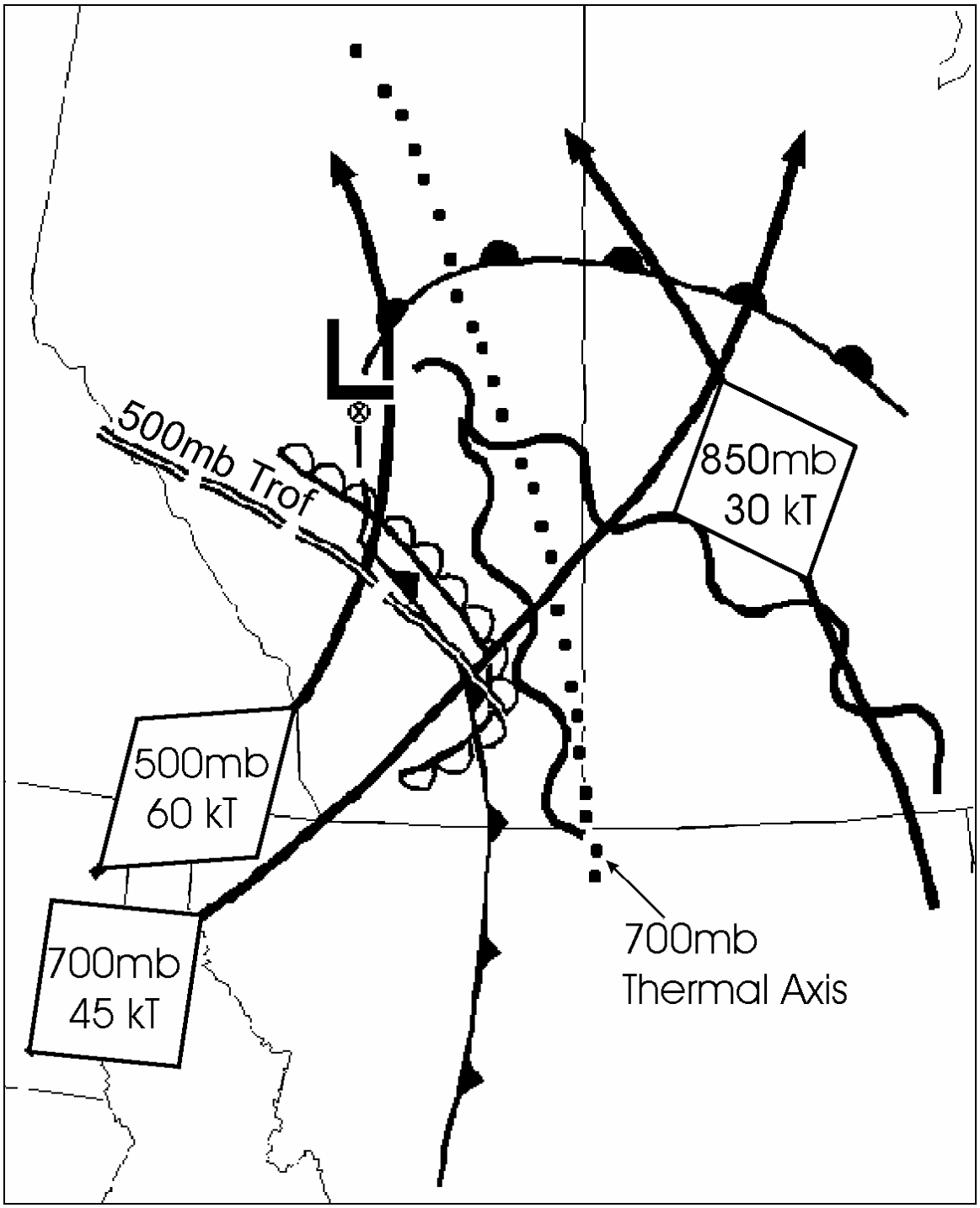

Figure 5: Composite figure at 0000 UTC 30 July 1993 showing the jet cores at 500mb, 700mb, and 850mb (arrows), the 500mb trof (double dashed line), and the 700mb thermal axis (dotted line). The location of the surface dryline, dewpoint temperature axis and fronts are indicated by the conventional symbols.

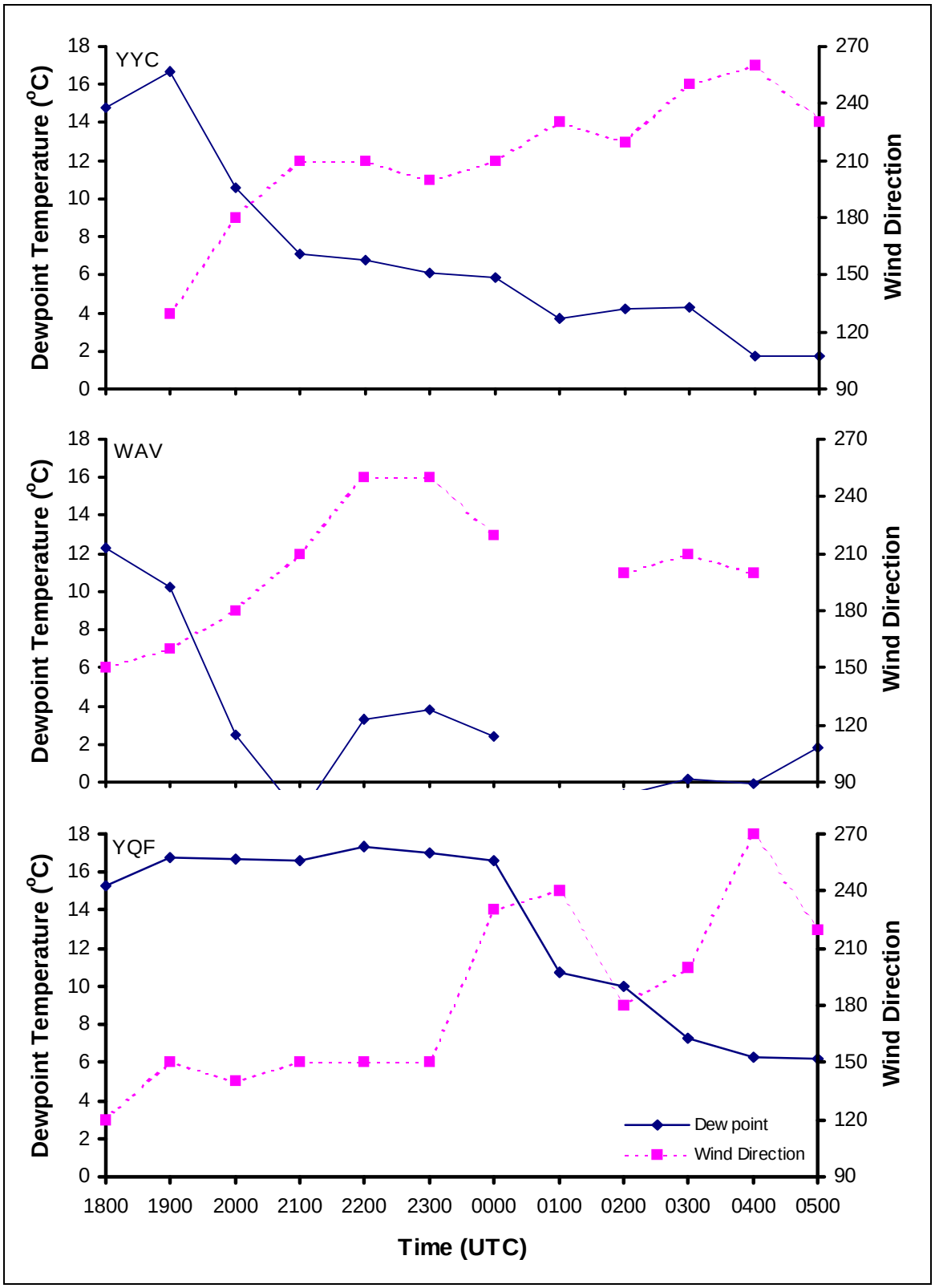

Figure 6: Temporal evolution of dewpoint temperature and wind direction for Calgary (YYC), Sundre (WAV), and Red Deer (YQF). Observations missing for WAV at 0100 UTC and dewpoint temeratures are below 0°C at 2100 UTC and 0200 UTC.

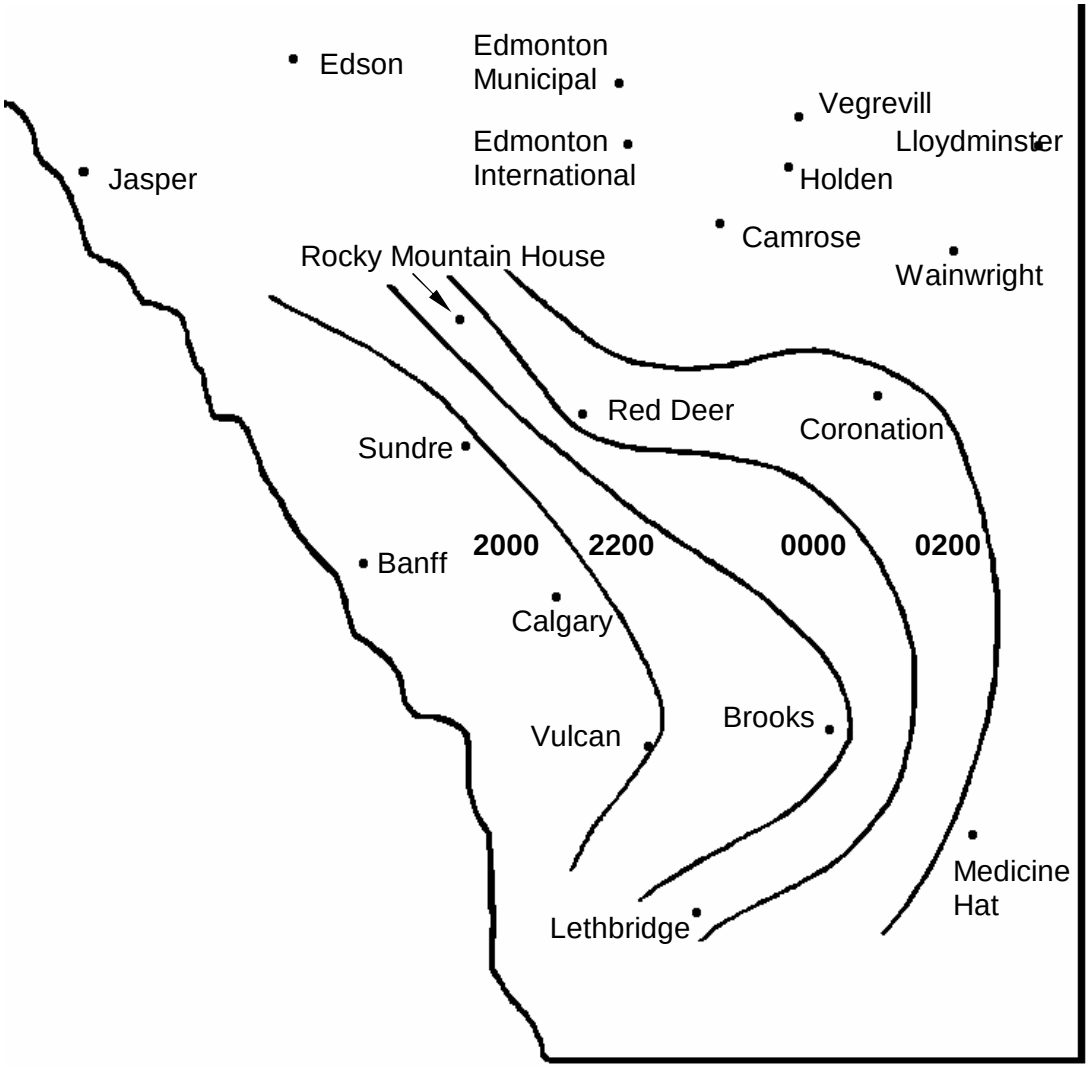

Figure 7: Alberta dryline evolution depicted by isochrones in 2 hour increments from 2000 UTC until 0200 UTC.

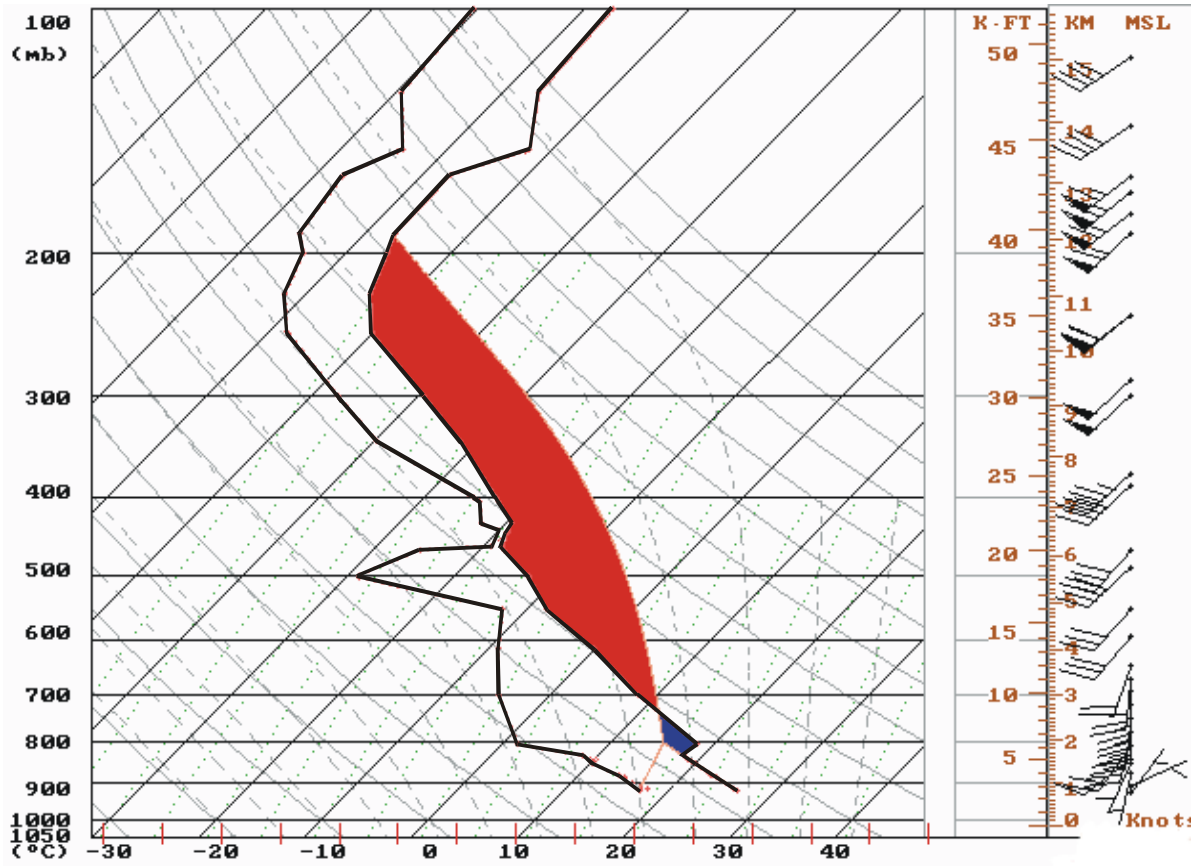

Figure 8: Skew-T Log P diagram from the 1200 UTC 29 July 1993 Stony Plain sounding using modified surface temperature and dewpoint of 26.2°C and 17.0°C, respectively. Buoyant energy is shaded and the wind profile is illustrated at right in knots.

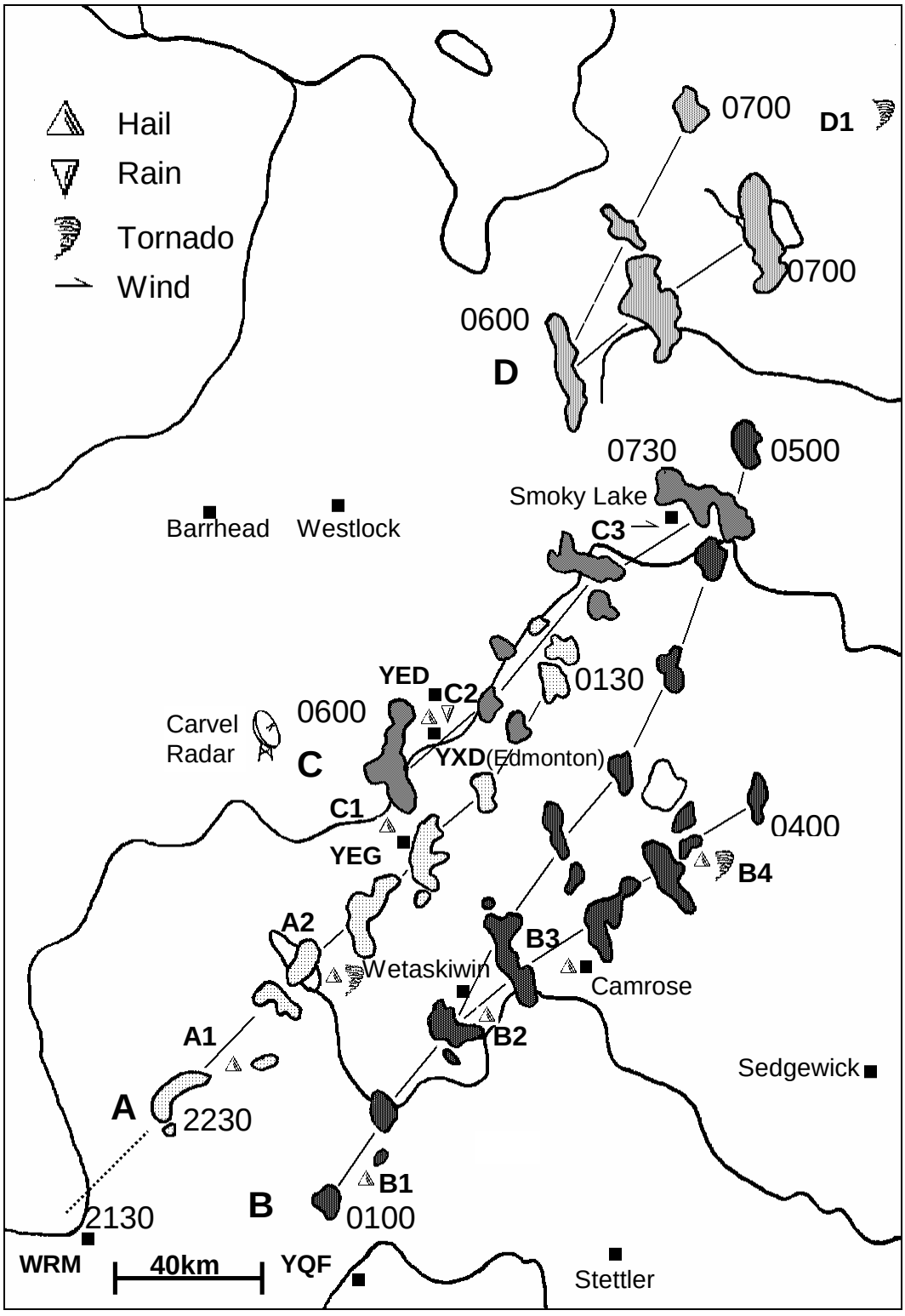

Figure 10: Composite storm tracks for 29-30 July 1993. The >52 dBZ core is contoured in 30 min intervals with all times in UTC. The storm tracks are labeled A, B, C, D corresponding to the Pigeon Lake, Holden, Edmonton, and Lac La Biche storms, respectively. The severe weather event markers are given in the upper left corner and the events are labeled as in Table 2.

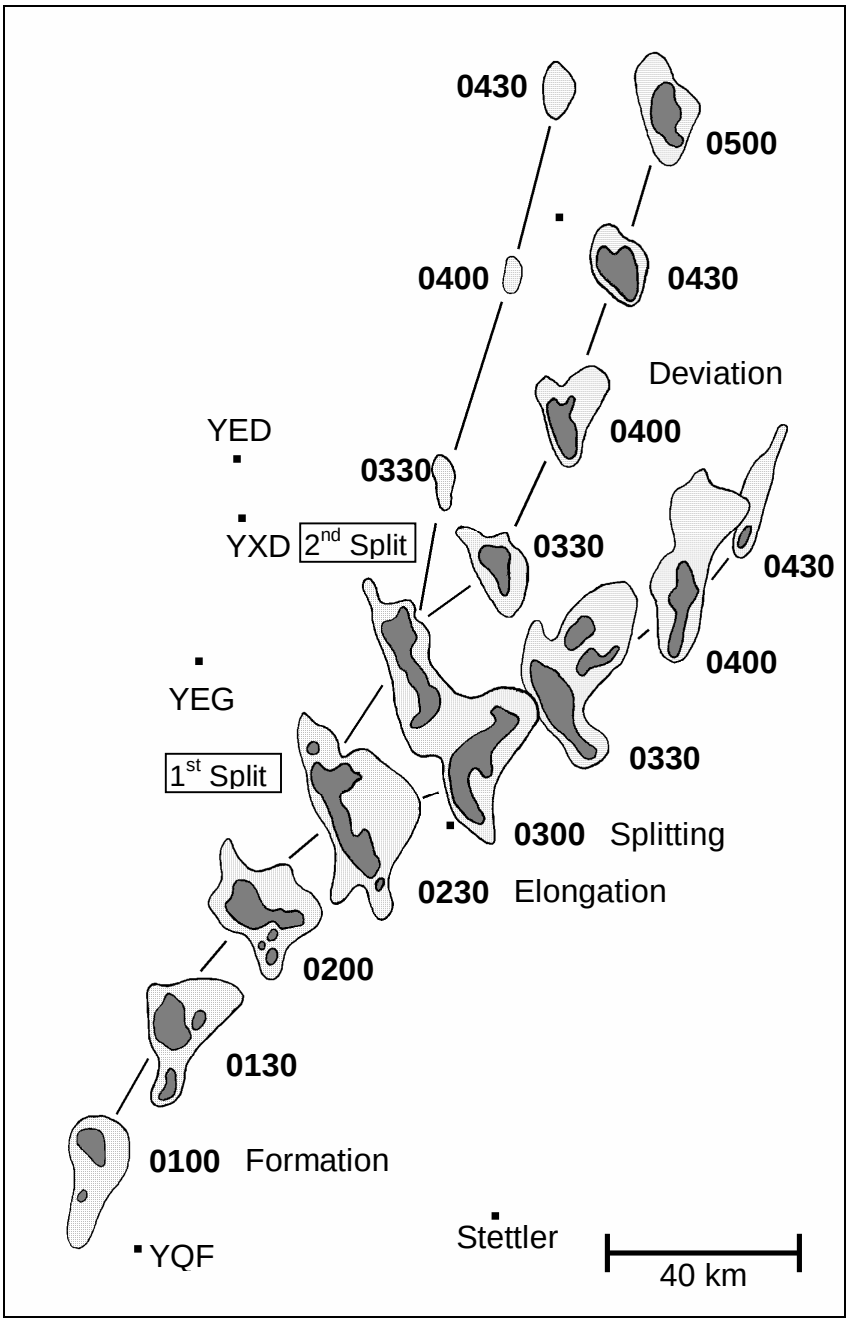

Figure 11: Storm tracks for the Holden splitting storm. The contours correspond to dBZ reflectivity values of 42 dBZ and ≥ 52 dBZ. The storm is contoured at 30 min intervals with all times in UTC.

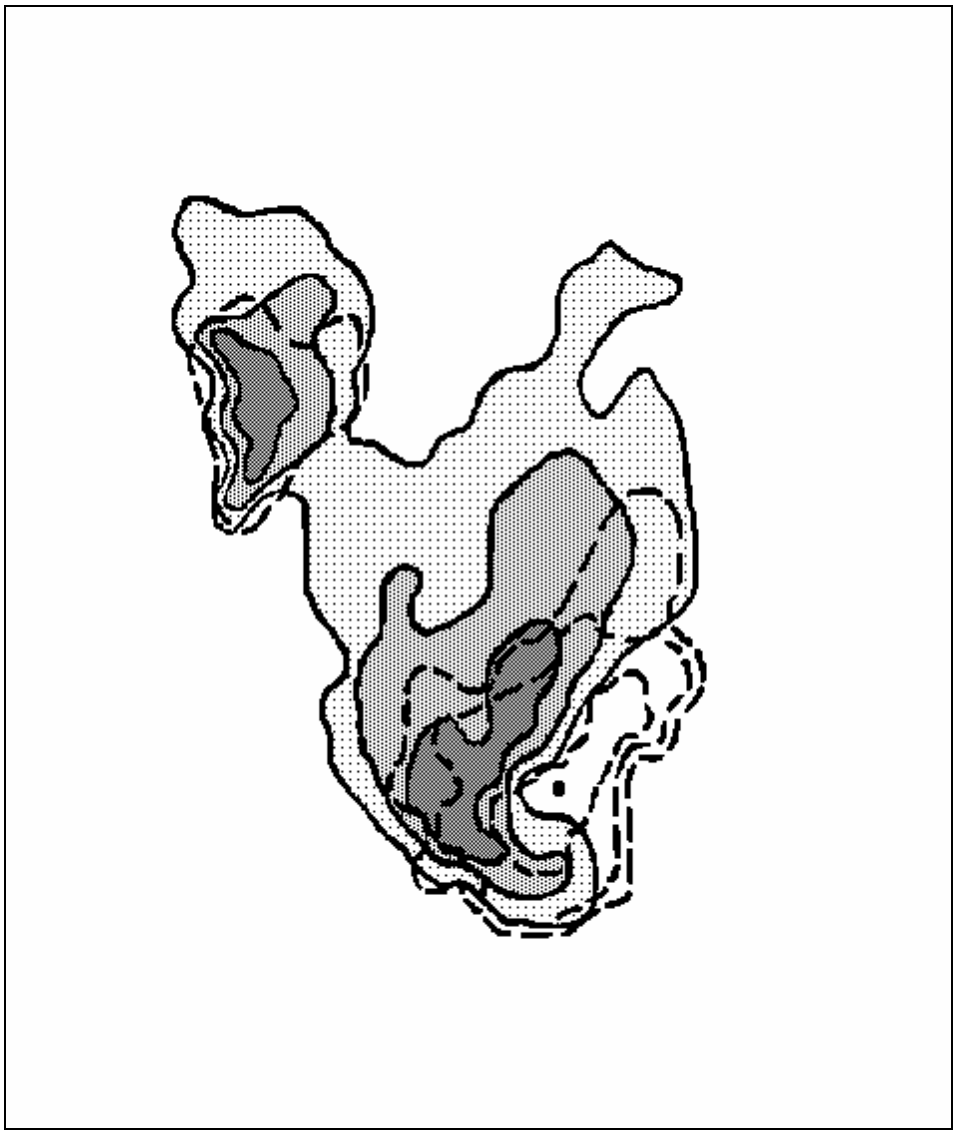

Figure 12: Composite radar image of the Holden storm at 0340Z (the approximate time the tornado was first sighted) showing 1.5km CAPPI reflectivities of 28 dBZ (lightly stippled), 42 dBZ (moderately stippled), and ≥ 52 dBZ (heavily stippled) and contoured heights of the 40 dBZ reflectivity (dashed) at 8.5km, 10.5km and ≥12km intervals. The approximate location of the storm top is indicated by a dot directly above the WER.

Table 1: Summary of severe weather events and their associated parent thunderstorms.

Storm / Event	Time (UTC)	Type	Location	Size / Intensity
A Pigeon Lake Storm				
A1	2245	Hail	Bluffton	Baseball
A2	2330	Hail	Pigeon Lake	Golfball
	0000	Tornado	Falun	F0
B Holden Storm				
B1	0130	Hail	Lacombe	Walnut
B2	0220	Hail	10km SE Wetaskiwin	Walnut
B3	0250	Hail	Camrose	Golfball
B4	0340	Hail	Ryley	Golfball
	0345-0405	Tornado	Holden	F3
C Edmonton Storm				
C1	0545	Hail	Devon	Walnut
C2	0610	Hail	Edmonton	Golfball
	0650	Rain	Edmonton	50 $mmhr^{-1}$
C3	0725	Wind	Smoky Lake	Structural Damage
D Lac La Biche Storm				
D1	0800	Tornado	60km NE Lac La Biche	F1

Table 2: Summary of the radar echo core evolution in 30 min intervals.

Time (Z)	Radar Echo Appearance
0100	· First echo >52 dBZ · Tight reflectivity gradient on right flank
0130	· > 52 dBZ cell (and entire storm) growing
0200	· 52 dBZ cell elongates perpendicular to mean wind · Still Z gradient on right flank · Weaker cell off left flank
0230	· Cell elongation ~ 30 km wide
0300	· Cells split, RM appears as classic supercell · Prominent WER on right flank of RM, hook echo later associated with F3 tornado touchdown near Holden · > 52 dBZ cells separated along axis perpendicular to mean wind
0330	· RM still stronger w/ WER
0400	· RM weakening · LM and RM separated by ~10 km
0430	· No detectable precipitation between LM and RM
0500	· RM dissipated, LM still echo > 52 dBZ